DOR: 20.1001.1.27170314.2022.11.4.5.7

Research Paper

# Thermal and Stress Analysis in Butt, T-shaped and Tubular Joints in the Welding Process of Dissimilar Parts

**Adel Tavabe[1], Behdad Jahanbeen[1], Seyed Mohammad Reza Nazemosadat[1], Ahmad Afsari[1*]**

[1]Department of Mechanical Engineering, Shiraz Branch, Islamic Azad University, Shiraz, Iran

[*]Email of the Corresponding Author: Ah.Afsari1338@iau.ac.ir

*Received: April 2, 2023; Accepted: May 21, 2023*

**Abstract**

Connecting parts through welding as permanent connections can play an important role in various industries. Despite the favorable load-bearing capabilities of joints resulting from welding dissimilar parts, they have some limitations that need to be identified and checked to optimize their use. One of the limitations is the behavior of parts under thermal stresses caused by the welding process. Thus, it is important to consider the welding conditions of the dissimilar parts in the contact area of the electrode and the welding seam, as this can significantly affect the mechanical performance of the welds. The research conducted in this study involved using the electric welding method with non-consumable tungsten electrodes under shielding gas (TIG) to connect aluminum and carbon steel parts. Ansys software was utilized to investigate the effect of thermal stress in the welding process for different joints. To ensure accuracy, parts were welded together practically under similar conditions, and the results obtained were compared with the results of the modeled method. First, the behavior of a steel sheet under the butt and Tee Joint and then the role of various factors on welding performance were investigated by modeling the process for a pipe in different conditions. Finally, due to the significant role of T-shaped joints in various industries, heat distribution, behavior, and stress analysis were investigated.

**Keywords**

Welding Process, Dissimilar Joints, Residual Stress, Thermal Analysis, Finite Element Method

## 1. Introduction

Tungsten Inert Gas (TIG) welding or arc welding with a non-consumable electrode covered with protective gases is an electric welding process. It involves the formation of an arc between the non-consumable tungsten electrode and the molten pool. Tungsten arc welding can be used with or without filler metal. In this process, there is no slag, so it is necessary to cover the electrode, crater, welded zone, and filler metal with shielding gas to prevent contamination and oxidization [1]. The welded joint and structure may undergo distortion and residual stress if the metal is restrained under heating and cooling. Several factors can increase the level of residual stresses and distortion in the welded joint, such as the degree of restraint, the design of the welded joint, the amount of preheating, and heat treatment after welding. Residual stresses can be changed with time and distance from the welding line. Transverse and longitudinal residual stress change at the pointed position is shown in

Figure 1. Blue and red lines named as σ1 and σ2 are related to high and low temperatures during and after welding respectively. Residual or remained stress can surpass yield stress and induce permanent deformation in the shape by introducing distortion (Figure 2) [2].

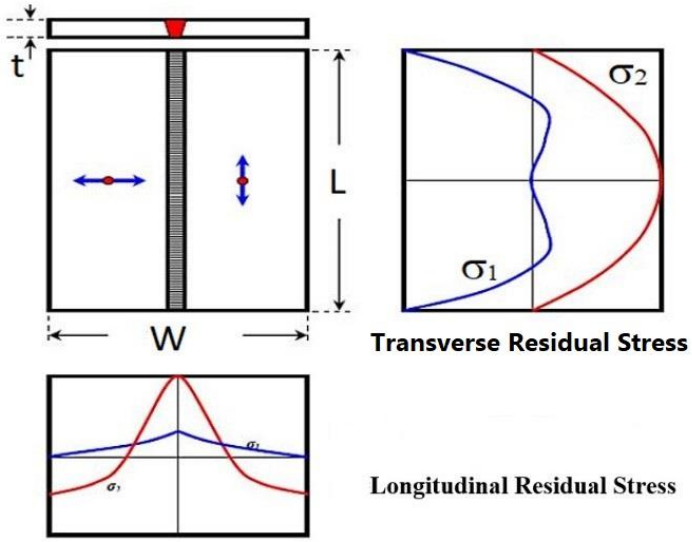


Figure 1. Residual stresses are caused by the welding process [2]

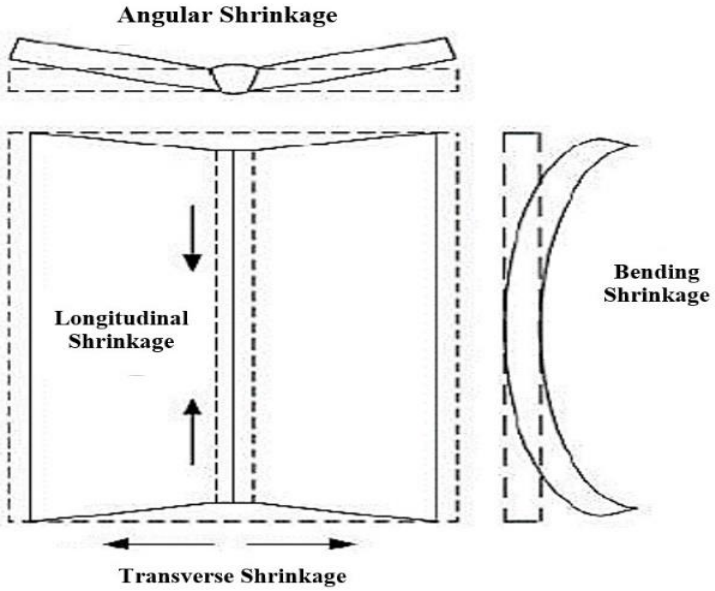


Figure 2. The change in structure form is due to residual stresses [2]

To minimize the distortion resulting from welding, the appropriate welding order, and sequence can be utilized without external restraints or jigs and fixtures. As fusion welding processes cause expansion and contraction, the joints can undergo distortion due to the differences in heat transferred to the base metal. One of the common methods to reduce the amount of shrinkage and distortion is multi-pass welding. By controlling the temperature between passes, multi-pass welds can reduce input heat and facilitate the use of an appropriate welding sequence and order [3]. Also welding passes and layers on both sides of the welding joint, creating a balance in its distortion (Figure 3).

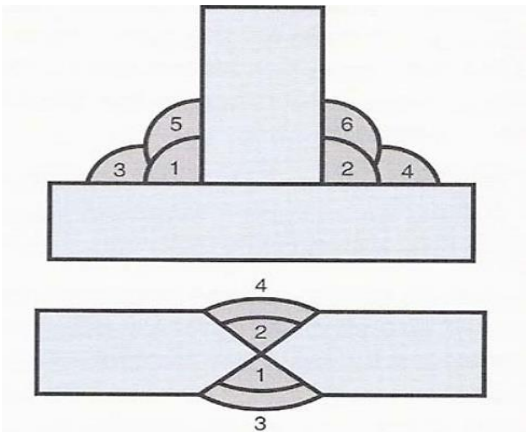


Figure 3. Order and sequence of welding [2]

Aluminum alloys are widely used in various industries due to their favorable properties. There are various methods employed for welding these alloys, with TIG welding being a commonly used one [4]. When aluminum is exposed to the atmosphere during welding, it develops an oxide layer on its surface, which has a melting temperature of approximately 1982 °C, higher than that of pure aluminum (660 °C). This oxide layer can reduce the welding ductility, so using a protective gas shield to prevent its formation can be beneficial. TIG welding is considered superior to other fusion welding methods for aluminum alloys because of its low density, high cooling rate, and the possibility of vertical and horizontal electric arc welding [5].

The thermo-mechanical behavior of the fusion welding process has been analyzed to determine the effect of weld fillets on the size and distribution of residual stress in dissimilar joints.

Increasing pipe wall thickness, particularly on the carbon steel side, leads to higher compressive axial residual stresses on the inner surface and axial tensile residual stresses on the outer surface [6]. Also, the numerical and experimental investigation of temperature and residual stress distribution in the multi-stage welding process of two stainless steel sheets with unequal thickness shows that numerical results and the experimental measurements are in good agreement with each other and the resulting model can make a good prediction of the temperature distribution and residual stress in the welding process [7]. Conventional fusion welding of dissimilar metals is often limited by the different thermal and physical properties of the parts to be joined. As a result, brittle intermetallic compound (IMC) phases may occur. Using a pressure welding process such as magnetic pulse welding (MPW) significantly reduces the risk of IMCs [8]. T-shaped joint fillet welds are widely used in ship engineering and bridge structures. Localized heating and subsequent rapid cooling of welding cause tensile residual stress near the toe of the T-joint in fillet welds, leading to structural distortion that affects the buckling strength of welded structures [9, 10]. Gas metal arc welding (GMA) is one of the most important metal joining processes due to its high productivity and compatibility with automation. This welding process is characterized by a complex V-shaped joint geometry, a deformable weld pool surface, and the addition of hot metal droplets [11].

Residual stresses from welding can be remarkably high, and they can reduce the strength of welded parts and even lead to cracks. In this research, the electric welding method with a non-consumable tungsten electrode under shielding gas (TIG) was used to connect T-shaped parts of aluminum and

carbon steel. Then the thermal analysis was done to obtain the thermal gradient by Ansys software and at the end, the analysis of the residual stress in the T-shaped joints was done.

## 2. Materials and Methods

### *2.1 Thermal analysis*

To determine the welding residual stresses, an initial thermal analysis must be conducted. The governing equation for heat transfer is represented by equation 1, [12]:

$$\rho_{C_p} \frac{\partial T}{\partial t} = \frac{\partial}{\partial X}\left(K \frac{\partial T}{\partial X}\right) + \frac{\partial}{\partial Y}\left(K \frac{\partial T}{\partial Y}\right) + \frac{\partial}{\partial Z}\left(K \frac{\partial T}{\partial Z}\right) + Q \qquad (1)$$

In this equation, ρ denotes the material density in kg/m3, Cp represents the specific heat capacity in J/(kg°k), T refers to the material temperature at a given moment in °k, and K is the temperature-dependent thermal conductivity in W/(m°k). Q refers to the internal production heat rate in W/m3 and t is the amount of time in seconds.

Since equation 1 is nonlinear, initial and boundary conditions are necessary to solve it. The material properties required for this thermal analysis include density, specific heat capacity, and thermal conductivity, which are provided for the material used in this research.

The pre-assumed conditions are: (a) the initial temperature of the part before welding is equal to the ambient temperature. (b) Equation for the heat flux applied by the welding electric arc on the workpiece surfaces considered to be the Gaussian heat distribution formula:

$$q = \frac{3Q}{\pi a^2} exp\left(-3\frac{r^2}{a^2}\right) \qquad (2)$$

where q, is the heat flux or intensity distributed on the surface of the part during welding, r is the distance from the center of the welding arc, and a is the radius of the circle to which about 95% of the heat flux is concentrated, and Q is the amount of input heat obtained from the following equation:

$$Q = \eta \times V \times I \qquad (3)$$

Where η, is the welding efficiency coefficient and its value depends on the type of welding and is obtained experimentally, V represents the voltage and I refers to the welding current.

Lastly, heat transfer occurring between the part's surfaces and the surrounding area through convection and radiation must also be taken into account. This heat exchange occurs for all surfaces of the boundary volume, except for surfaces that are welded together. The equations for these two types of heat transfer are represented as follows [13]:

For convection heat transfer:

$$q_c = h_c(T - T_\infty) \qquad (4)$$

For radiant heat transfer:

$$q_r = h_r(T - T_\infty) \qquad (5)$$

$$h_r = \sigma\varepsilon F\left(T^2 + T_\infty{}^2\right)(T + T_\infty) \quad (6)$$

In equations 4 and 5, $q_c$ refers to the heat transferred by displacement, $h_c$ represents the displacement thermal conductivity coefficient, $q_r$ denotes the heat transferred by radiation, $h_r$ is the radiation heat transfer coefficient, σ represents the Stefan-Boltzmann constant, ε denotes the emission coefficient, and F is the shape coefficient or surface factor.

*2.2 Stress analysis*

During the welding process, the material undergoes plastic strain due to the rapid increase in temperature and low yield stress at high temperatures. Therefore, to accurately analyze the behavior of the material and calculate residual stress, it is essential to utilize thermos-elastoplastic relationships.

$$[d\sigma] = [D^{ep}]\{d\varepsilon\} - \left[D^{th}\right]\{dT\} \quad (7)$$

Where dσ and dε and dT are stress, strain, and temperature derivative, $[D^{th}]$ is the thermal stiffness of matrix and $[D^{ep}]$ is equal to the sum of $[D^e]$ and $[D^p]$, which are respectively the elastic and plastic stiffness of matrix. Since the strains created in welding are a function of thermal history and loading, this equation is written in fraction form [13]. The value of dε can be written as follows:

$$\{d\varepsilon\} = \{d\varepsilon^e\} + \{d\varepsilon^p\} + \{d\varepsilon^{th}\} + \{d\varepsilon^{ph}\} - \{\alpha\}\, dT - (T - T_\infty)\,\{d\alpha\} \quad (8)$$

Where $\{d\varepsilon^e\}$, $\{d\varepsilon^p\}$, $\{d\varepsilon^{th}\}$ and $\{d\varepsilon^{ph}\}$ are the derivatives of elastic, plastic, thermal, and phase change strains respectively, and $\{\alpha\}$ is the coefficient of thermal expansion, which is dependent on the temperature.

To numerically solve the equations related to stress analysis, it is enough to determine the mechanical properties of the material.

Then by incorporating thermal analysis results, the residual stress values can be obtained. To determine the value of the plastic strain derivative $\{d\varepsilon^p\}$, it is necessary to have information about the standard yield stress and strain hardening history [14]. The experiment shows that the real behavior of the material is a state between two types of isotropic and kinematic strain hardening. The effect of strain hardening on residual stress distribution is studied. One of the critical material characteristics to determine is the yield stress at any temperature, which changes as the temperature varies during the welding process.

*2.2 Experimental method*

In this research, the input parameters of current, voltage, welding speeds, thickness, and material of the welded part were used for thermal analysis in welding joints. After determining the input parameters and performing the operation at certain points, the output results of temperature distribution were recorded and the temperature was measured in a practical way using a calibrated thermometer device (Figure 4). The welding process was carried out using a 250 amp welding rectifier and an air-cooling torch from the Iranian Industrial Development Company (Figure 5).

Green-colored tungsten electrodes with Russian welding wire aluminum filler and shielding gas with a combination of 80% Co2 and 20% Argon were used. The torch was held at an angle of 75 degrees to create an electric arc between the electrode and the workpiece.


Figure 4. Thermometer device (temperature measurement)

Figure 5. Pictures of welding machine and argon torch

Filler metal was also used and it was heated under an angle of 15 degrees by a welding torch and then fed into the molten pool. The polarity was determined based on the type of metal being welded, alternating current (AC) was used for aluminum, and direct current with reverse polarity was used for steel or other metals. Initially, two dissimilar sheets made of aluminum 5052 alloy and carbon steel S235JR, each with a length, width, and thickness of 200, 130, and 10 mm respectively, were prepared for butt joints (Figure 6). Quantum testing was performed on both pieces to ensure their chemical composition, and the mechanical characteristics of the steel and aluminum sheets were presented in Tables 1 and 2, respectively.

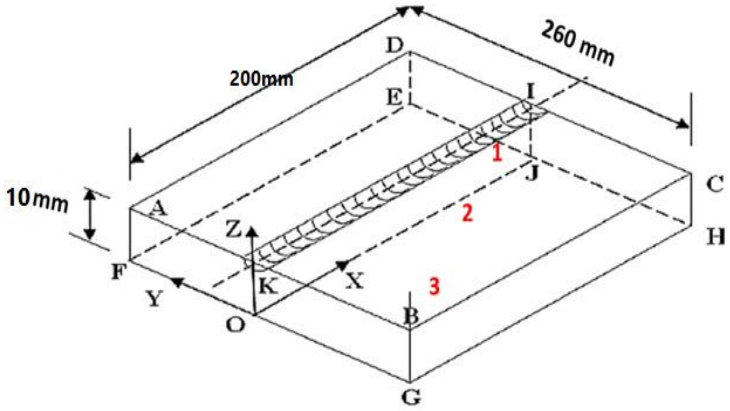


Figure 6. Dimensions of parts used in welding and simulation operations. Welding Starts from right to left

The prepared parts were attached and welded together using the TIG welding method with a current of 120, 140, and 160 amps and a constant voltage of 12 volts, a welding speed of 4 mm/s, and an ambient temperature of 32°C. The results of temperature distribution were constructed by the thermometer. This welding operation was finished after 50 seconds and the temperature was measured at different positions according to Figure 6 in the first 5, 25, and 50 seconds of welding. Results of practical and simulated temperature at points 1,2 and 3, are presented in Table 3.

Table 1. Mechanical characteristics of steel sheet

| **Mechanical Property** | **Units** | **Value** |
|---|---|---|
| Thermal conductivity coefficient | $w\,m^{-1}C^{-1}$ | 51.1 |
| Specific heat capacity | $j\,k\,g^{-1}C^{-1}$ | 450 |
| Poisson's ratio | - | 0.3 |
| Young's modulus | $G\,p\,a$ | 200 |
| Convection heat transfer coefficient | $w\,m^{-2}C^{-1}$ | 6.5 |
| density | $k\,g\,m^{-3}$ | 7894 |

Table 2. Mechanical properties of aluminum

| Mechanical property | Units | Value |
|---|---|---|
| Thermal conductivity coefficient | $w\,m^{-1}C^{-1}$ | 138 |
| Specific heat capacity | $j\,k\,g^{-1}C^{-1}$ | 860 |
| Poisson's ratio | - | 0.3 |
| Young's modulus | $G\,p\,a$ | 70 |
| Convection heat transfer coefficient | $w\,m^{-2}C^{-1}$ | 6.5 |
| density | $k\,g\,m^{-3}$ | 2782 |

Further, to investigate the behavior of different materials under the effect of heat caused by the welding process, the joint of two dissimilar pipes made of aluminum alloy 5052 and carbon steel S235JR has also been investigated. Table 4 shows the comparison of temperature at current values of 120, 140, and 160 amps for both simulation and practical methods with a constant voltage of 20 volts and a constant welding speed of 10 millimeters per second at the tubular specimen. The welding operation was completed after about 20 seconds.

Table 3. Temperatures variation in the first 5, 25, and 50 seconds for butt joints at positions 1, 2, and 3 of steel

| The recording status of temperatures measured | Position 3 | | Position 2 | | Position 1 | |
|---|---|---|---|---|---|---|
| | practical | simulation | practical | simulation | practical | simulation |
| In the first 5 seconds | 20 | 20 | 240 | 244 | 474 | 468 |
| In the first 25 seconds | 20 | 20 | 237 | 230 | 443 | 440 |
| In the first 50 seconds | 20 | 20 | 220 | 218 | 426 | 417 |

Table 4. Comparison of temperature with current changes in simulation model with the practical process for tubular specimen on steel side

| Welding Steps | Current (amps) | Voltage (Volt) | Speed mm/s | Temperature (°C) | |
|---|---|---|---|---|---|
| | | | | Simulation | Practical |
| W01 | 120 | 12 | 10 | 270-300 | 286 |
| W02 | 140 | 12 | 10 | 320-350 | 341 |
| W03 | 160 | 12 | 10 | 370-400 | 393 |

Investigation of thermal stress in welding with T-shaped joints of the dissimilar joint of aluminum AL5052 with carbon steel S235JR was continued. The dimensions of the aluminum and steel parts are shown in Figure 7. Here, the welding process was carried out on three samples, and in each piece, 3 positions at 1,3, and 5 cm distances from the weld line were selected and temperature changes with time were recorded. Dimensions of sheet again selected as 200*130*10 mm similar to butt welding but in T-shaped orientation. The comparison of temperature changes according to Figure 7 at positions 1 and 2 of samples A, B, and C is presented in Tables 5 and 6.

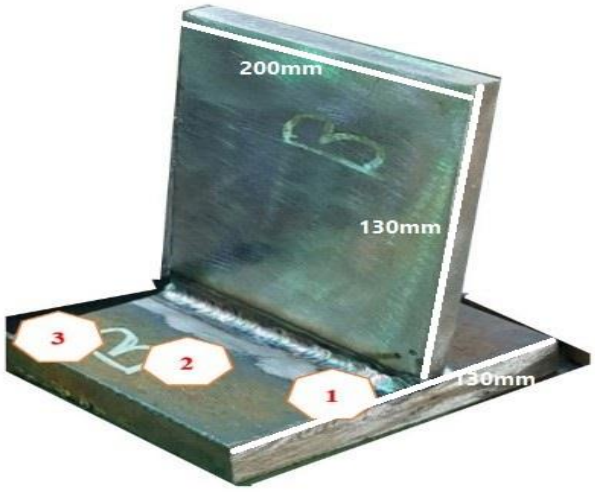


Figure 7. Points 1, 2, and 3 were selected for temperature measurement

Table 5. Comparison of temperature changes at point 1 of samples A, B, and C with T-shaped joint

| Time (s) | Analysis Methods | | | |
|---|---|---|---|---|
| | Sample A | | Sample B | Sample C |
| | Simulation | Practical A | Practical B | Practical C |
| 0-10 | 128 | 125 | 125 | 118 |
| 10-20 | 25 | 26 | 29 | 28 |
| 20-30 | 26 | 24 | 25 | 25 |
| 30-40 | 24 | 24 | 23 | 23 |
| 40-50 | 22 | 20 | 22 | 22 |

Table 6. Comparison of temperature changes in point 2 of samples A, B, and C with T-shaped joint

| Time (s) | Analysis Methods | | | |
|---|---|---|---|---|
| | Sample A | | Sample B | Sample C |
| | Simulation | Practical | Practical | Practical |
| 0-10 | 25.05 | 25.3 | 23.3 | 24 |
| 10-20 | 25.1 | 25.5 | 24.7 | 25.1 |
| 20-30 | 25.5 | 26.4 | 25.5 | 27.2 |
| 30-40 | 25.5 | 28.6 | 25.7 | 29.3 |
| 40-50 | 25 | 24 | 24.7 | 25.5 |

The results for point 3 are almost similar to point 2. In T shaped joint maximum temperature of point 1 on the steel plate is much lower than in the butt joint. Higher thermal conduction of the aluminum part accompanying heat release pattern change related to T-shaped orientation induced lower heat input and related temperature on the steel side.

## 3. Results and discussion

In this section, the behavior of welded joints in different working conditions will be investigated. As mentioned, in this part, the behavior of a weld in the joining of two sheets in butt weld orientation has been simulated numerically, and its results have been compared with the existing values. In the next step of solving the problem, the appropriate mesh is created on the sheet according to Figure 8. As it is known, organized and finer meshing has been used in the areas near the bead to increase accuracy. In Figure 9, the location of the heat source is also shown. During the simulation, the movement of the heat source from the beginning to the end of the path is fully considered. As was said before, to ensure the correctness of the numerical solution, it is necessary to verify the obtained results.

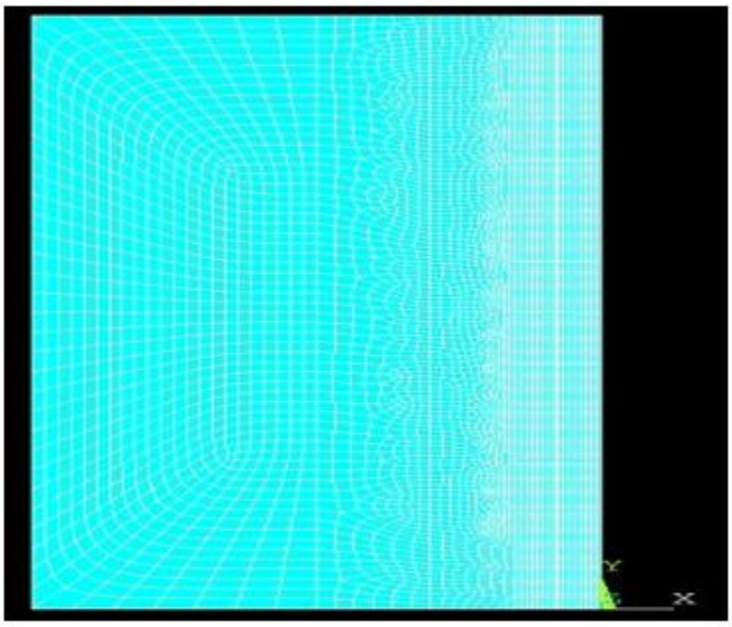

Figure 8. Front view of the network created on the surface of the sheet

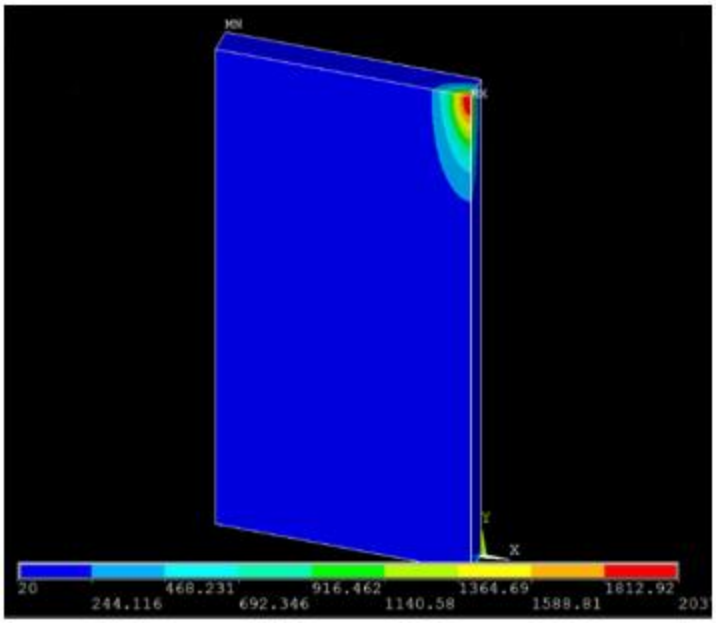


Figure 9. Heat distribution on the sheet surface in 5 seconds

Figure 10 shows the graph of temperature variation was obtained from numerical analysis midway on seam weld with 150 mm distance from the start point and compared with the practical results obtained. As it is known, the obtained results of the numerical analysis have a very good match with the practical results, which indicates the accuracy and effectiveness of the numerical solution. One of the other important steps that should be considered in numerical analysis is selecting suitable meshing. The purpose of this analysis is to ensure that the mesh is fine enough for the independence of the results with the size of the mesh elements. For this purpose, the maximum temperature in the mentioned sheet was obtained according to the size of different mesh elements, and its results are presented in Figure 11. As it is clear from the results obtained in this section, by making the mesh size ratio bigger than 1, the results showed almost no changes, which showed the convergence of the solution. Overall, the results from this section demonstrated a high level of accuracy and provide valuable insights into the behavior of welded joints in different working conditions.

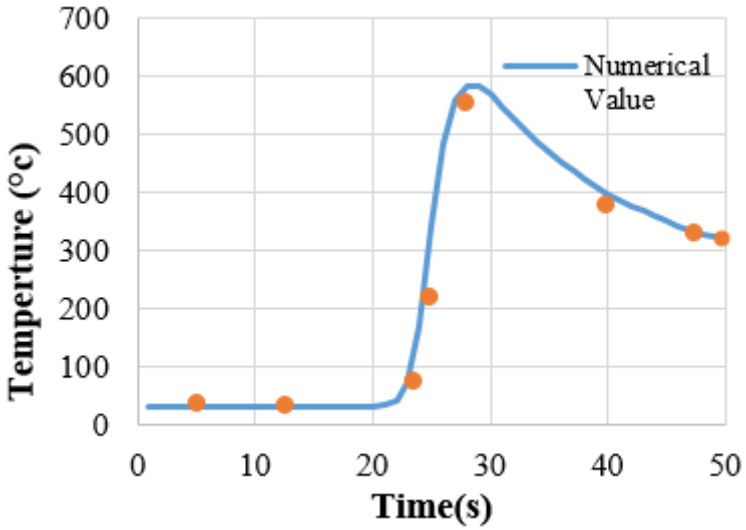


Figure 10. Comparison of the numerical method and practical values of the Temperature-Time variation on seam weld of a butt joint midway of welding

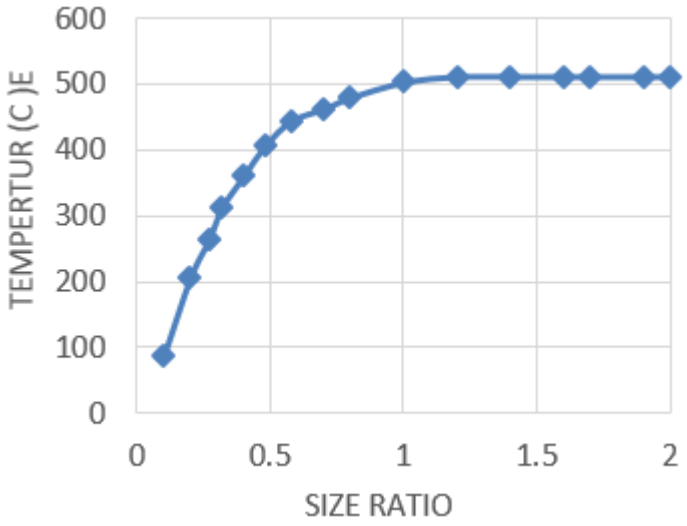


Figure 11. Examining the effect of grid size on maximum temperature

*3.1 Effect of electric current*

One of the factors that influence welding quality is the source of electrical energy. To investigate this effect on electric current, a tube with a thickness of 10, a length of 260, and a radius of 32 mm was analyzed as depicted in Figure 12. A suitable meshing was created on the surface, as shown in Figure 13. In this case similar to butt and T-shaped joints welding of the similar sheet with dimensions of 130×200×10 mm but after rolling analyzed. Next, three different welds on the pipe surface were simulated and analyzed according to Table 7. In this simulation, an attempt was made to determine the temperature distribution dependency around the weld seam with current, and the results are presented in Figure 14.

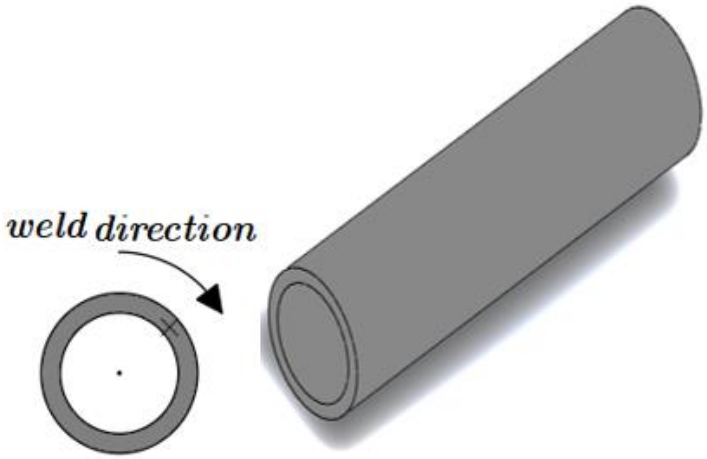


Figure 12. View of the considered pipe model

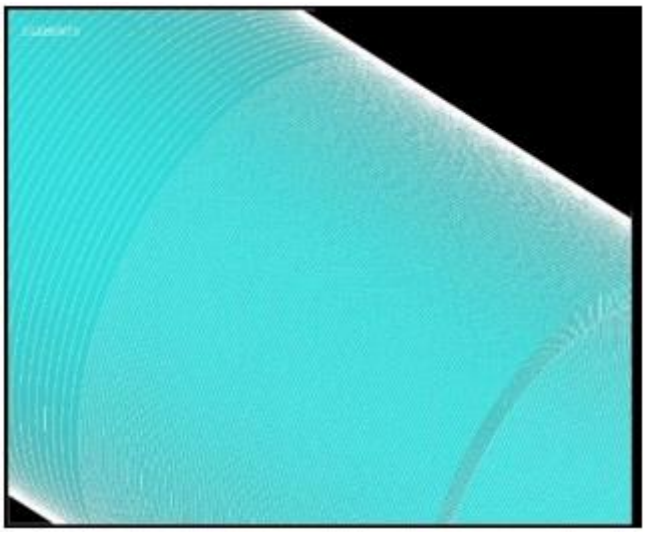

Figure 13. The network created on the pipe surface

Table 7. Weld modeling parameters in pipe model with variable current

| Weld number | Current (A) | Voltage (V) | Speed (mm/s) | Welding time (s) | Max Temperature |
|---|---|---|---|---|---|
| 1 | 120 | 12 | 10 | 20 | 288 |
| 2 | 140 | 12 | 10 | 20 | 341 |
| 3 | 160 | 12 | 10 | 20 | 393 |

As illustrated in Figure 14, an increase in the current and source power at constant welding speed will lead to an increase in the heat input per unit length of weld and maximum temperature near the weld seam, so for a 33% increase in the electric current, a 37% increase in the maximum temperature has been observed in the model. This amount of temperature increase shows the determining role of the energy source on the quality and performance of welding. An increase in temperature due to its effect on cooling rate, can also lead to an increase in residual stresses in the weld joints.

Figure 15 shows the temperature distribution on the surface of the model for tubular welding. Also in this figure, the melting zones, the partial melting zone(PMZ), and the heat-affected zone (HAZ) are well shown. As it is known, in the melting zone, the temperature has increased to approximately 620 °C.

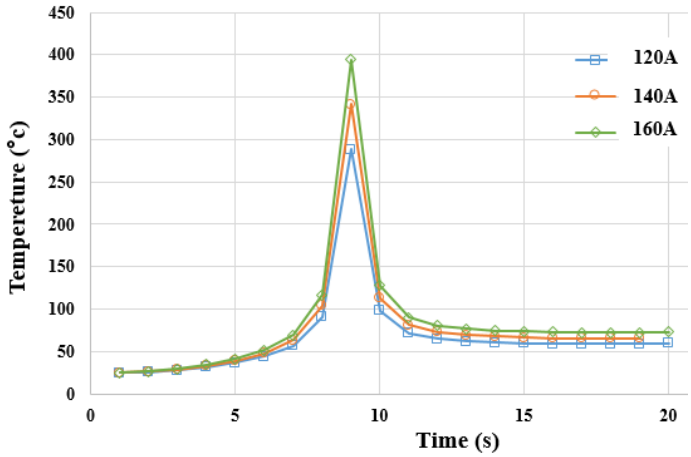


Figure 14. Temperature changes for a point around the weld seam with variable current at tubular modeling and welding speed of 10 mm/s

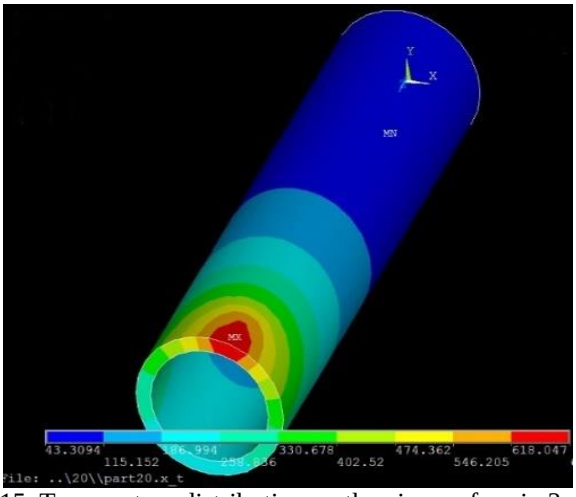


Figure 15. Temperature distribution on the pipe surface in 3 seconds

*3.2 Effect of welding speed*

In Figure 16, the changes of residual stress near the weld seam are shown, and as can be seen, the stresses are initially compressive, but over time, the stresses become tensile, and after a certain time of about 12 seconds, the stress will reach to a constant compressive value of 60 MPa. This value can greatly affect the mechanical behavior of the joints and lead to the failure of the joint at far lower compressive loads than the design loads.

The maximum temperature changes at a point near the weld seam of T shaped joint have been investigated for different welding speeds. The values considered in this case are given in Table 8 and Figure 17. As shown in Figure 17, with the increase in the welding speed, the simulation total welding time decreased and the maximum temperature shifted to lower times. The maximum temperature is generally not affected by welding speed but at higher welding speed related to low heat input per length of weld, the change in thermal conductivity reduces thermal transfer and slightly increases the maximum temperature. These outcomes imply that the welding speed is crucial in the welding process since this parameter not only affects the maximum temperature but also the residual stresses in the weld.

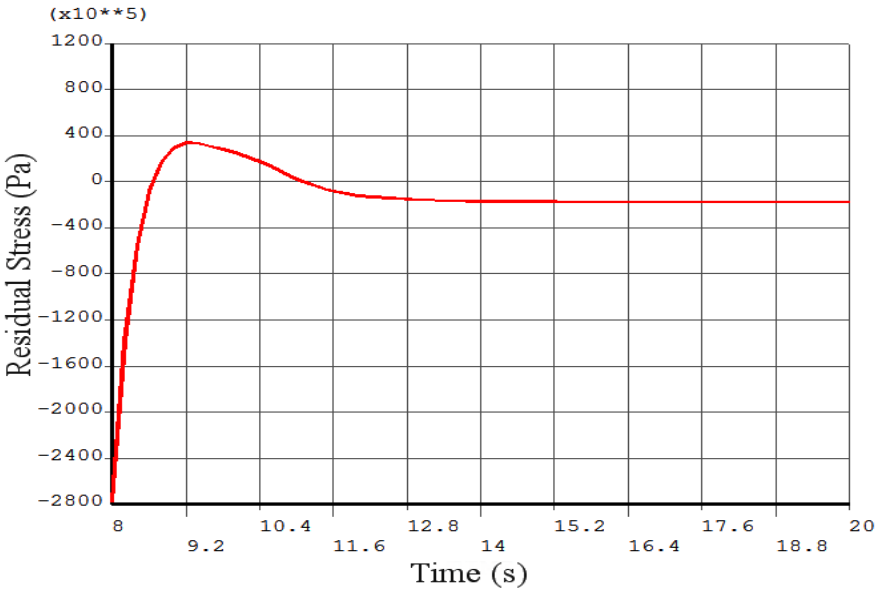


Figure 16. Residual stress changes with Time around the weld seam in the tubular joint

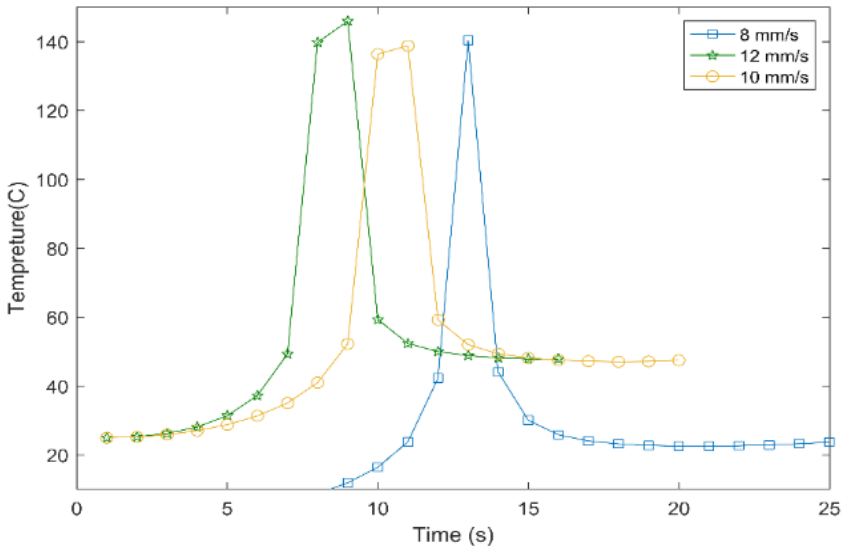


Figure 17. Temperature changes around the weld seam with variable welding speeds at Tubular shaped joint on the Al side

Table 8. Welding modeling parameters in the Tubular shaped joint with variable welding speeds

| weld number | current (amps) | Voltage (V) | Speed (mm/s) | Welding time (seconds) |
|---|---|---|---|---|
| 1 | 160 | 12 | 8 | 25 |
| 2 | 160 | 12 | 10 | 20 |
| 3 | 160 | 12 | 12 | 16 |

Increasing welding speed at a constant current can decrease heat input per length of weld thus increasing the cooling rate and increasing remaining thermal stress. Figure 18 shows the variation of remaining thermal stress at different welding speeds with time at the seam weld position. At welding speeds of 10 and 12 mm/s initial tensile stress at the seam line is very higher than in 8 mm/s. Cracking occurring in the center line will be promoted at higher cooling rates. Increasing the distance from the seam weld line decreased internal stress and changed it to compressive. At far enough distance, Stress

tends to be about zero or somehow slightly tensile type, and increasing welding speed increased the final stress. Thus residual stress after cooling at the center of the seam weld is tensile but compressive at positioned far from the weld line.

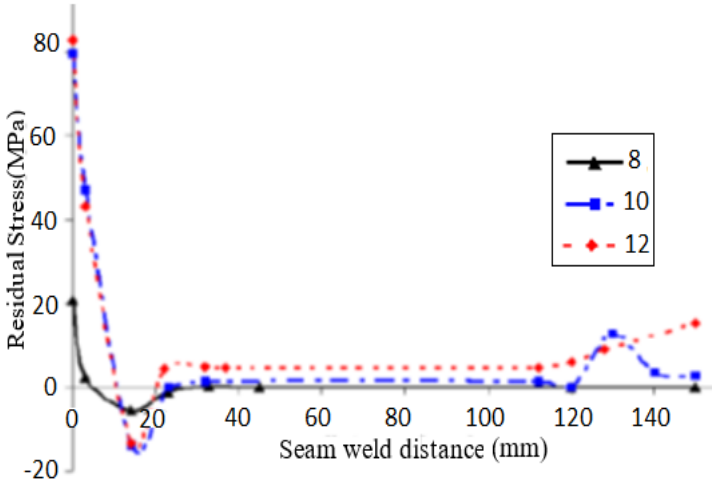


Figure 18. Variation of residual stress with distance and welding speed at seam weld of Tubular shaped joint

According to Table 9, by increasing the welding speed magnitude of maximum longitudinal and transverse residual stress increased. Maximum residual stress in the transverse direction is lower than longitudinal and the increase of 33% in welding speed conducted to 3.5% and 11% increase in the Longitudinal and transverse side that is far below the 37% increase in Maximum temperature. Residual stress is affected by heat input per length of weld and cooling rate. Heat input per length or Maximum temperature potentially increases the residual stress but cooling rate can reduce or reverse this phenomenon. So in low heat input always the residual stress will be negligible but in high heat input conditions only when the cooling rate is enough slow, the residual stress can be reduced.

Table 9. Welding speed effect on maximum remained Stress

| Welding speed (mm/s) | 8 | 10 | 12 |
|---|---|---|---|
| Longitudinal Stress (MPa) | 245 | 247 | 254 |
| Transverse Stress (MPa) | 138 | 145 | 153 |
| Equivalent Von Misses Stress (MPa) | 239 | 242 | 253 |

### *3.3 Results of the dissimilar pipe welding*

Figure 19 shows the temperature in steel and aluminum pipes at different periods. As it is clear from the results, the maximum temperature on the steel side of the pipe is much higher than the Aluminum side of the pipe, which is due to the higher thermal conductivity coefficient in aluminum compared to steel. The maximum temperature in the steel sheet is approximately equal to 580 °C. While this value on aluminum side is equal to 345 °C. which is approximately 40% lower than the maximum temperature calculated for steel. This temperature difference will lead to a difference in the mechanical behavior of the pipe. This temperature difference will induce different strains on both sides of the pipe, and this shows the necessity of considering thermal stresses in the design and installation of supports.

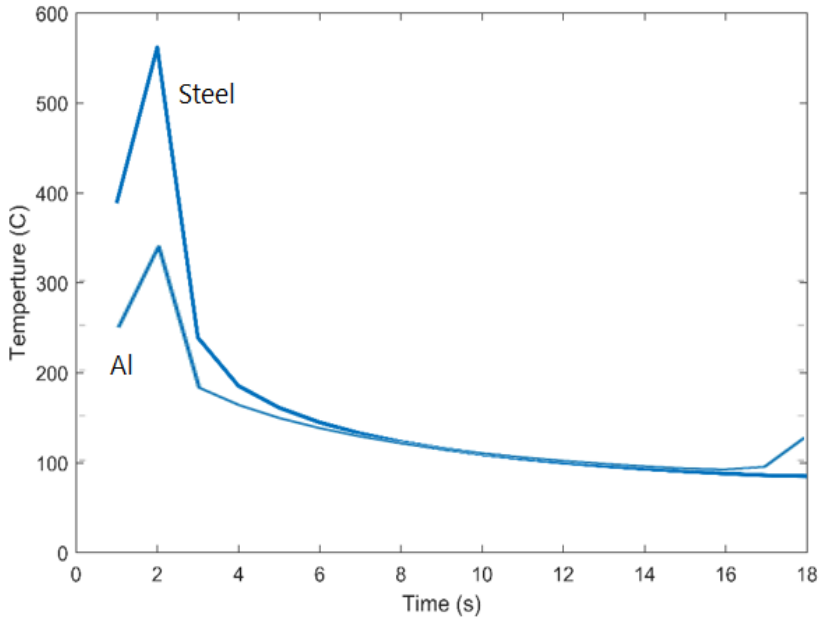


Figure 19. Temperature changes over time in aluminum and steel sides of tubular joints

*3.4 Temperature distribution in the T-shaped joint*

In the continuation of the simulation, the behavior of a T-shaped joint was investigated. T-shaped joints are widely used in various industries due to their wide functionality and high load-bearing capacity. The appropriate mesh was created on the model, which is shown in Figure 20, and as it is clear, to reduce the solution time and also the accuracy of the calculations, the number of elements in the bead area was chosen much smaller. In addition, due to the large temperature gradient in this area, the increase in the number of elements will lead to an increase in the accuracy of the calculations, in this regard the temperature distribution at different times is shown. Figure 21 shows the contours of temperature distribution after 34 seconds. As it is clear in the figures, over time, the temperature will increase in the entire joint surface, which can lead to permanent deformations in the joints and create residual stresses.

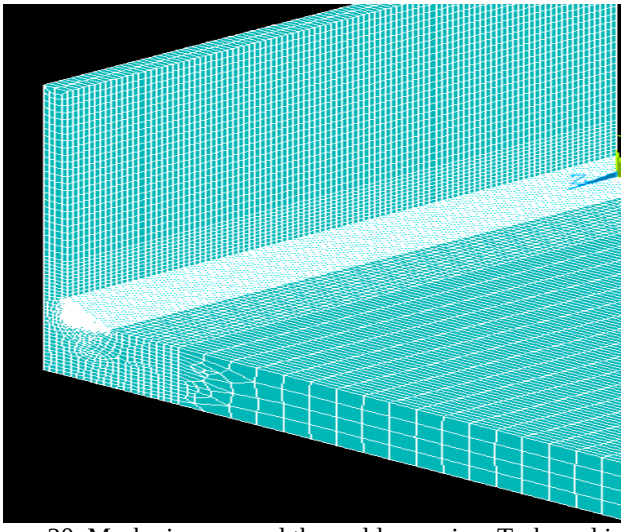

Figure 20. Mesh view around the weld seam in a T-shaped joint

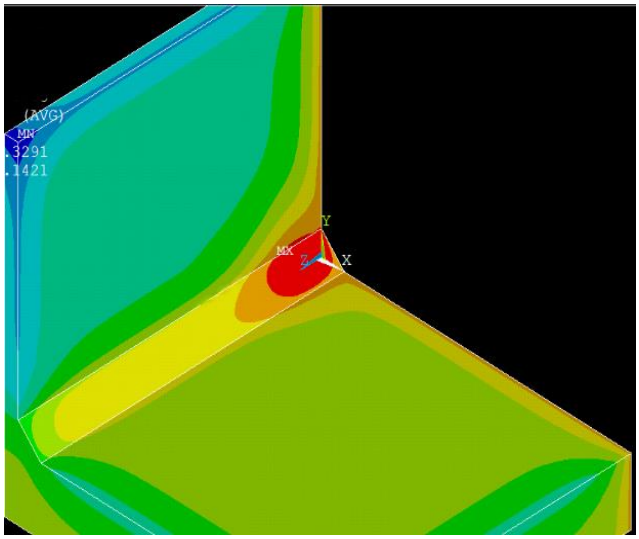


Figure 21. Temperature distribution in the T-shaped joint after 34 seconds

Figure 22 shows the temperature change with time for point 1 of Figure 7 and Table 5. The temperature has increased to 128 degrees Celsius while the temperature of points 2 and 3 almost has not changed with welding. These points are located at a greater distance from the welding line and, as is clear are less affected by the heat caused by the welding process.

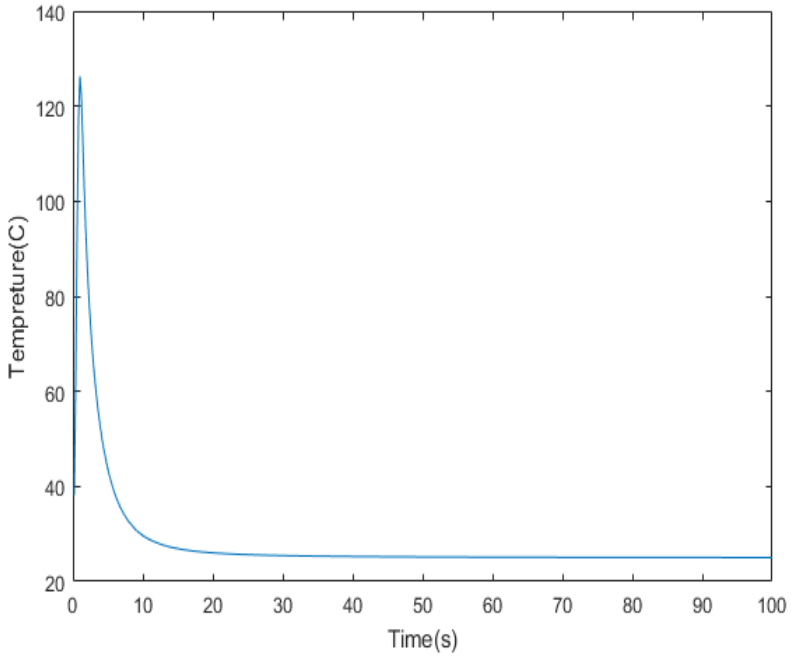


Figure 22. Temperature changes in terms of time at point 1 of Figure 7 in a T-shaped joint

*3.5 Discussion of the residual stress of the T joints*

Different welding parameters such as total heat input, heat intensity or heat input per length, welding method, welding speed, yield stress, and material elasticity and plasticity modulus can affect the residual stress value and its distribution. In the areas close to the bead, the temperature at the root of the weld reaches about 1500 °C and in the center of the main branch, the temperature decreases to about 444 °C. Points far from the bead do not tolerate many changes. From the temperature-time

changes in Figure 22, it can be seen that the speed of temperature rising or heating rate during welding is higher than the speed of temperature drops or cooling rate after welding. The stress values and the contour of the longitudinal and the transverse stress distribution which are given in the sheet-by-sheet model are observed (Figures 23 and 24).

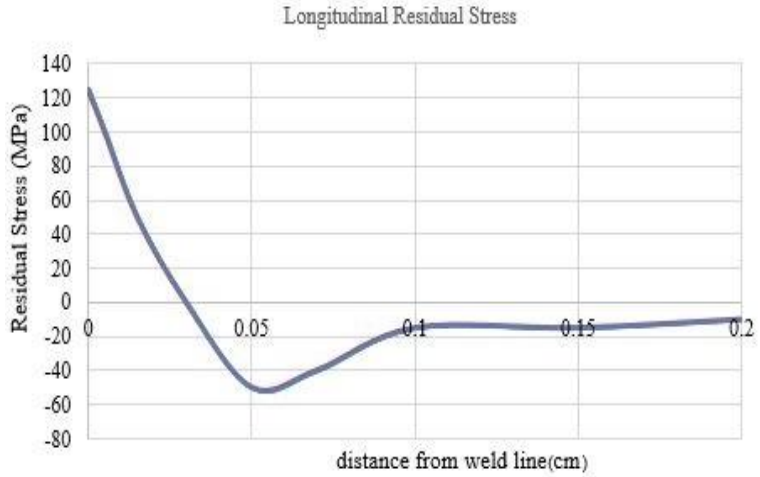


Figure. 23. Longitudinal residual stress diagram perpendicular to the welding line of the butt joint

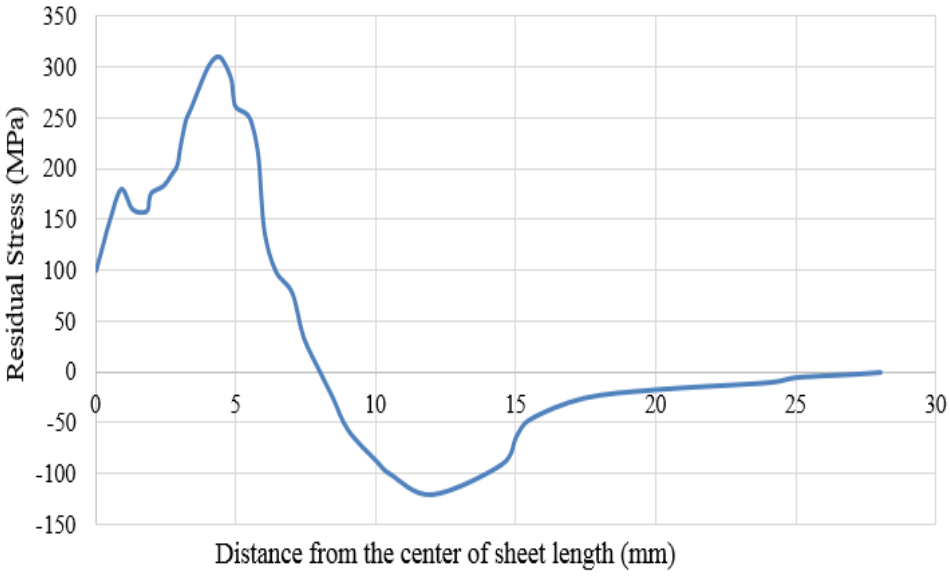


Figure 24. Transverse maximum residual stress diagram parallel to the welding line of butt joint

Figure 25 shows the comparison of residual stress results of finite element modeling with experimental ones. In the graphs of Figure 25, it shows that the stress in the weld and near the weld is tensile and by moving away from the central line of the weld, the stresses move towards compression. Also, according to the diagram in Figure 25, in the direction perpendicular to the weld line and near it, large amounts of tensile residual stress are generated. This type of stress gradually appears towards the edges of the sheet in the form of compressive stresses. In the direction parallel to the welding line and at the edges of the sheet, the stresses are compressive, while in the central region, the stresses appear tensile. At the point below the electrode, where the molten pool is formed, the stresses are compressive, and after passing the electrode and passing the heat flux through that area, the stresses move towards tensile. Figure 24 depicts residual transverse

stress for specified distances from the weld line, indicating that the stress initially increases up to 5 mm and then decreases until it tends to zero after a 15 mm distance of the weld line in T-shape modeling. The accuracy of results can be influenced by different welding parameters, metallurgical and mechanical properties, as well as thermal properties of materials.

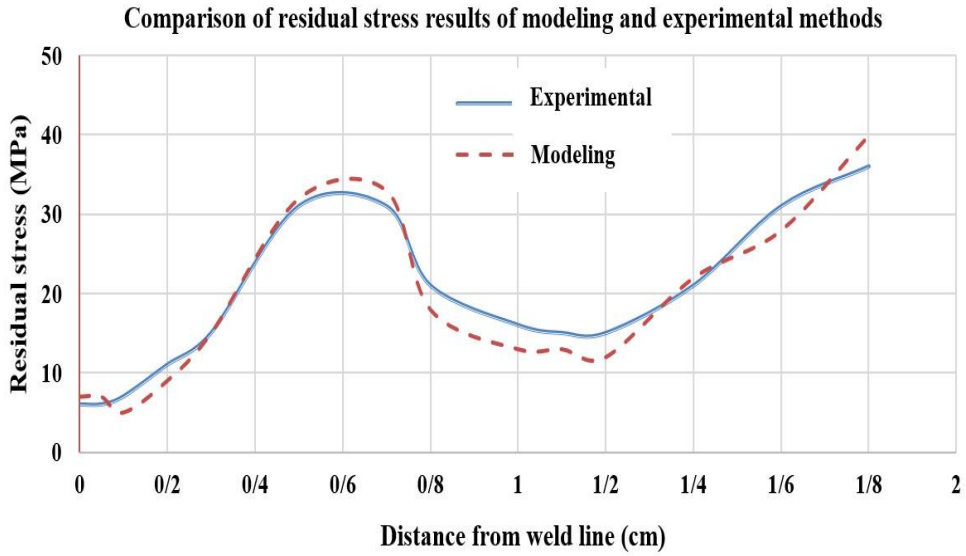


Figure 25. Comparison of modeling and experimental residual stress results at different distances to weld line

Based on the selection of the number of mesh elements, the amount of heat input, the method of applying the heat flux, the welding speed, and the amount of the yield stress, the amount and distribution of the stress can be affected.

It is worth noting that by moving away from the central line of the weld, the stresses tend towards compression. The stresses are compressive in the direction parallel to the welding line at the edges of the sheet, while the central region shows tensile stresses. In the direction perpendicular to the weld line and near it, large amounts of tensile residual stress are generated, which eventually becomes compressive towards the edges of the sheet.

According to this figure, the experimental and numerical results are in good agreement with each other; Of course, there are differences between experimental results and finite element modeling (measurement of stress at a distance of one centimeter from the weld seam with experimental results) in terms of whether the stress is tensile or compressive. This issue can be due to residual stress measurement errors and the cleaning process. Although small differences in welding parameters, welding conditions, metallurgical and mechanical properties, and thermal properties of materials can also affect the accuracy of the results.

## 4. Conclusion

This research investigates the TIG welding process of Aluminum and steel and its impact on temperature and thermal stresses in different Joint types using Ansys software and numerical analysis. Initially, a steel sheet's behavior under the butt joint was studied. Next, the influence of various factors on the welding performance of tubular joints was analyzed by model. Finally, T-shaped joints were

examined. In each case, 3 points at different distances from the weld line were selected for stress and temperature measurement and its comparison with experimental results.

• The temperature decreased with increasing distance from the weld line and there was good compatibility between calculated and measured temperatures

• Rate of heating was higher than the rate of cooling and the temperature on the steel side was always higher than the aluminum side on all joint types due to the higher thermal conductivity coefficient of aluminum.

• According to the findings, by increasing heat input per length, the peak temperature near the weld seam increased significantly. A 40% increase in electric current leads to approximately a 37% increase in the peak temperature. The peak temperature is also affected by the thermal conduction of material which itself is temperature dependent.

• Initially, residual stresses around the pipe were compressive but eventually become tensile. At a far distance from the welding seam, the stress values tend to be about 60 MPa in a compressive state. Residual stress is a function of heat input and cooling rate and increasing heat input decreases but increases as the cooling rate increases. At lower heat input always residual stress values are small but at high heat input, the cooling rate will be determining and control parameter on residual stress.

• Longitudinal residual stress in butt welding at the weld line was tensile but by increasing distance from the weld line decreased and changed to compressive and eventually tend to zero.

Transverse residual stress in butt welding at weld line, stress is tensile and by increasing distance from weld line decreased and changed to compressive like as Longitudinal stress but maximum stress is not located al weld line

• The maximum temperature increased with an increase in welding speed but does not significantly affect stress increase.

• In T-shaped joints, the heat impact on the model increases due to the two welding passes executed simultaneously. The study found that longitudinal residual stresses near the weld have tensile values and reach compressive values as they move away from the weld line. The comparison of finite element modeling residual stress results with experimental findings showed that the experimental and numerical results correspond well.

• Maximum temperature is always measured on the steel side and in the butt joint and T-shaped joints have the highest and lowest values. These differences arise due to orientation. In T shape joint there is another extra path for the dissipation of heat so the lowest temperature appeared.

## 5. References

[1] Parmar, R. S. 2001. Welding processes and technology. Khanna Publishers, India.

[2] Masubuchi, K. 2013. Analysis of welded structures: residual stresses, distortion, and their consequences. Elsevier.

[3] Marques, E.S., Silva, F.J. and Pereira, A.B. 2020. Comparison of finite element methods in fusion welding processes-A review. Metals. 10(1):75.

[4] Seok, C.S., Suh, M.W. and Park, J.H. 1999. Investigation of welding residual stress of high tensile steel by finite element method and experiment. KSME International Journal.13:879-885.

[5] Tschirner, P., Hillers, B. and Graser, A. 2002. A concept for the application of augmented reality in manual gas metal arc welding. International Symposium on Mixed and Augmented Reality, IEEE.

[6] Akbari, D. 2017. Effect of edge preparation on residual stress of welding in dissimilar joints. Modares Mechanical Engineering. 17(7):307-315.

[7] Nakhodchi, S., Akbari Iraj, S. and Rezazadeh, H. 2014. Numerical and experimental study of temperature and residual stress in multi-pass welding of two stainless steel plates having different thicknesses. Modares Mechanical Engineering. 14(9): 81-89.

[8] Bellmann, J., Schettler, S., Schulze, S., Wagner, M., Standfuss, J., Zimmermann, M., Beyer, E. and Leyens, C. 2021. Improving and monitoring the magnetic pulse welding process between dissimilar metals. Welding in the World. 65:199-209.

[9] Teng, T.L., Fung, C.P., Chang, P.H. and Yang, W.C. 2001. Analysis of residual stresses and distortions in T-joint fillet welds. International Journal of Pressure Vessels and Piping, 78(8), pp.523-538.

[10] Perić, M., Tonković, Z., Rodić, A., Surjak, M., Garašić, I., Boras, I. and Švaić, S. 2014. Numerical analysis and experimental investigation of welding residual stresses and distortions in a T-joint fillet weld. Materials & Design. 53:1052-1063.

[11] Zhang, W., Kim, C.H. and DebRoy, T. 2004. Heat and fluid flow in complex joints during gas metal arc welding-part I: numerical model of fillet welding. Journal of applied physics. 95(9):5210-5219.

[12] Ghassemi, H. 2011. Study of welding temperature history by dual reciprocity boundary element method. Modares Mechanical Engineering. 11(3):95-102.

[13] Majzoobi, G.H., Seifi, R. and Ali-akbar, S. 2012. Experimental and numerical study of temperature distribution and determination of residual stresses due to welding of plates. Journal of Modeling in Engineering. 9 (27): 49-59.

[14] He, B. 2005. Computer modeling of weld joint microstructure and residual stresses. PhD Thesis. Carleton University.